Proceedings of the XVII ECSMGE-2019
Geotechnical Engineering foundation of the future
ISBN 978-9935-9436-1-3

doi: 10.32075/17ECSMGE-2019-0998

XVII European Conference
ECSMGE 2019
Reykjavik
on Soil Mechanics
and Geotechnical Engineering

Desiccation and cracking behaviour of clayey soils: experimental characterization and mechanisms identification

Fissuration des sols argileux par dessiccation: caractérisation expérimentale et identification des mécanismes

A. El Hajjar
LOMC/UMR CNRS 6294/University Le Havre, Le Havre, France

T. Ouahbi, J. Eid, S. Taibi
LOMC/UMR CNRS 6294/University Le Havre, Le Havre, France

S. Bouchemella
INFRARES/Civil engineering department/University Souk Ahras, Souk Ahras, Algeria

J. Eid
Civil engineering department/Holy Spirit University of Kaslik (USEK), Jounieh, Lebanon

ABSTRACT: In our present society, raw earth presents an efficient alternative as an energy-saving building material to cope with climate and environmental issues. Nevertheless, it has a sensitivity to water, due to the presence of fines, which has a direct effect on its consistency. This can be expressed during desiccation, by shrinkage strains resulting in cracking that begins once the internal tensile stresses developed, due to suction, exceed the tensile strength of the material. In this work, using digital image correlation (DIC) technique, the evolution of the strain of clay samples, from the beginning of shrinkage until the initiation of cracks is treated. In order to understand the origin of cracking, desiccation is studied for different boundary conditions and according to the intrinsic characteristics of the material.

RÉSUMÉ: Dans notre société actuelle, la terre crue présente une alternative comme matériau de construction non énergivore pour faire face aux enjeux climatiques et environnementaux. Néanmoins, elle présente une sensibilité à l'eau, due à la présence des fines, qui a un effet direct sur sa consistance. Celle-ci peut se traduire lors d'une dessiccation, par des déformations de retrait aboutissant à la fissuration qui s'amorce une fois que les contraintes de traction internes développées, dues à la succion, dépassent la résistance de traction du matériau. Ce travail traite, par corrélation d'images numériques, l'évolution de la déformation d'échantillons argileux, dès le début du retrait et jusqu'à l'amorce de la fissure. Afin de comprendre l'origine de la fissuration, la dessiccation est étudiée pour différentes conditions aux limites et en fonction des caractéristiques intrinsèques du matériau.

Keywords: clayey soil; shrinkage; strain; cracking; digital image correlation.

1 INTRODUCTION

The raw earth is an old construction material which has a renewed interest and evolves quickly in recent years due to its low gray energy, its thermal inertia, as well as its almost immediate availability. Nevertheless, it has a sensitivity to water, due to the presence of fines, which has a direct effect on its consistency (El Hajjar et al., 2018).

The evaporation of water from the pores results in a shrinkage deformation, defined by a decrease in the volume of soil, which causes meniscus to

form around the soil particles. The relationship between the radius of curvature of the spherical water-air meniscus and the pressure difference between air and water is given by Laplace's law, which can be simplified in the case of cylindrical pores and take the expression of Jurin's law:

$$u_a - u_w = \frac{2\,\sigma_s \cos(\theta)}{r} \qquad (1)$$

with u_a and u_w : air and water pressures (Pa)
σ_s : water-air surface tension (N/m)
θ : connection angle between the meniscus and the solid (°)

(In the case of water, we have: $\sigma_s = 72{,}75.10^{-3}$ N/m and cos θ = 1, because the liquid-solid and the liquid-air surface tension of water are energetically more favourable than the solid-air surface tension).

This relationship implies that, at the meniscus, the water pressure is lower than the air pressure, especially since *r* is small (Delage & Cui, 2000).

This pressure difference, presented by suction, can lead to crack formation, that begins once the developed internal tensile stresses, due to suction, exceed the tensile strength of the material (Kodikara et al., 2000).

To remedy this problem, it is essential to understand the evolution of the deformation of the material during drying. This work presents an experimental study, which consists in carrying out free shrinkage tests on two types of clays (swelling and non-swelling) in order to identify the deformation leading to cracking according to the imposed boundary conditions, the heterogeneity of the sample and its intrinsic characteristics.

2 MATERIALS AND METHODS

2.1 Materials

The materials used are on the one hand a greek calcium montmorillonite and on the other hand a kaolinite called P300. Their geotechnical characteristics are presented in Table 1. Figure 1 shows a scanning electron microscope (SEM) observation as well as an X-ray diffraction (XRD) analysis (in powder form) of this montmorillonite. We notice that it shows a rather complex texture.

Table 1: Geotechnical characteristics of Greek calcic montmorillonite and P300 kaolinite (Fleureau et al., 1993).

Characteristic	Symbol	Mont.	Kaol.
Granulometry	< 80 µm (%)	100	100
	< 2 µm (%)	40	60
	d_{50} (µm)	4	1,5
Plasticity	w_L (%)	170	40
	w_P (%)	60	21
	I_p (%)	110	19
Grain density	Gs (g/cm^3)	2,73	2,65

A SEM image and XRD analysis (oriented blade) of P300 kaolinite are presented in Figure 2. It should be noted that this clay, which is in the form of rigid hexagonal platelets of varying sizes between 1 and 2 µm, contains in addition to kaolinite (peaks at 7,18 and 3,58 Å), illite (peaks at 10 and 5 Å) and quartz (peaks at 4,26 and 3,34 Å).

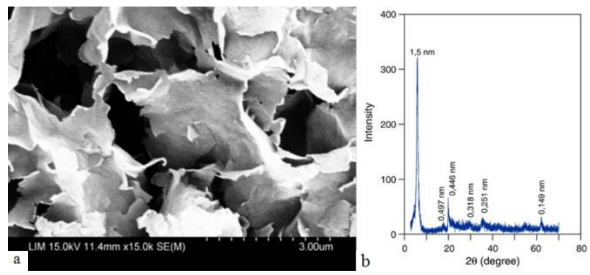

Figure 1: SEM observation (Hammad, 2010) (a) and XRD analysis of Greek calcic montmorillonite (Souli et al., 2008) (b).

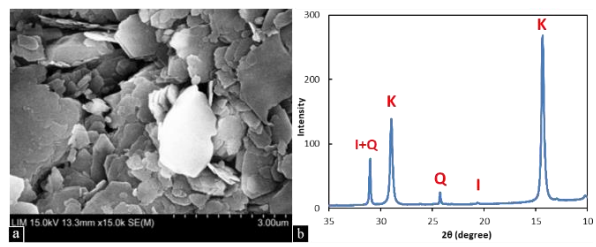

Figure 2: SEM observation (Hammad, 2010) (a) and XRD analysis of P300 kaolinite (b).

2.2 *Methods*

To study the effect of boundary conditions (external friction) on clay cracking, three different types of bases were pasted on a PVC plate:

a- Rough base: waterproof sandpaper having a very coarse grain “180” (commonly used for heavy stripping).

b- Semi-Rough base: waterproof sandpaper having a fine grain “400” (commonly used for finishing).

c- Smooth base: 1 mm thick virgin Teflon roll (static coefficient of friction = 0,08 to 0,10 according to ASTM D1894).

All samples have dimensions of 20 x 20 cm and a thickness of 8 mm, and are wetted at an initial water content of 1,5w_L (w_L : Liquid Limit) for the kaolinite and 1,35w_L for the montmorillonite. A speckled appearance, made with a white and black PVC powder, is required to allow the digital image correlation software to properly detect the difference between pixels. The entire experimental setup is controlled in terms of temperature (T = 22,5 °C) and relative humidity (RH = 18 %).

During drying, a *Canon 600D* camera with a Macro lens took a monochromatic grayscale picture every 10 minutes. The lighting is performed using two fluorescent lamps (cold light) to prevent any disturbance of the ambient temperature. A schematic diagram of the assembly of this device is shown in Figure 3.

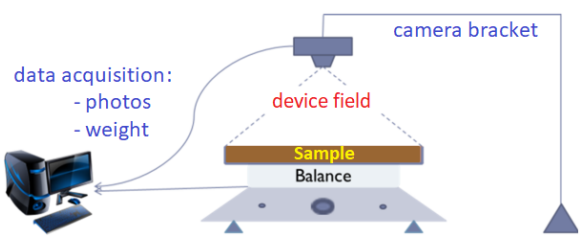

Figure 3: Schematic diagram of the experimental device (Eid et al., 2015).

To study the strain of sample, a digital image correlation software "VIC-2D" was used. This software analyzes the difference between the pixels in the photos taken, in order to obtain a two-dimensional strain field of the sample surface. On the other hand, crack morphology analysis is performed using the software "ImageJ" to measure the cracking and shrinkage surface of the samples in order to obtain the deformation density defined by the deformed surface (cracked and shrunk) divided by the total surface area of the sample in its initial state.

The tests carried out are presented in Table 2:

Table 2: List of samples

Sample number	Type of clay	Type of base
Sample 1	Kaolinite	Rough
Sample 2	Kaolinite	Semi-Rough
Sample 3	Kaolinite	Smooth
Sample 4	Montmorillonite	Rough
Sample 5	Montmorillonite	Semi-Rough
Sample 6	Montmorillonite	Smooth

3 RESULTS AND DISCUSSION

3.1 *Continuous strain*

On the drying path, the end of the experiment is reached when the residual water content of the sample becomes stable by forming a horizontal step on the curve of the evolution of the water content over time (Figure 4). The residual water content of the montmorillonite samples is 15,7 % while the residual water content is 0,6 % for the kaolinite samples.

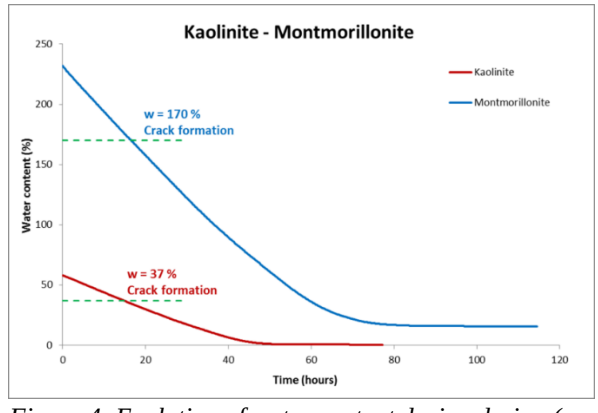

Figure 4: Evolution of water content during drying (on a rough base).

The difference in residual water content is due to the physical properties and crystallographic structure of the clay matrix. The matrix of montmorillonite has a large hydrated part in the form of bound water that requires a temperature of 200 °C to evaporate, and crystalline water that does not leave the paste until temperatures above 550 °C (Wakim, 2005). In addition, the slope of the montmorillonite drying curve (-3,7 %/hours) is twice as steep as that of the kaolinite (-1,4 %/hours).

Figures 5 and 6 show that kaolinite has only cracked on the rough base; while montmorillonite has cracked on all types of bases, undergoing a very high three-dimensional shrinkage and significant vertical deformations (Figure 7).

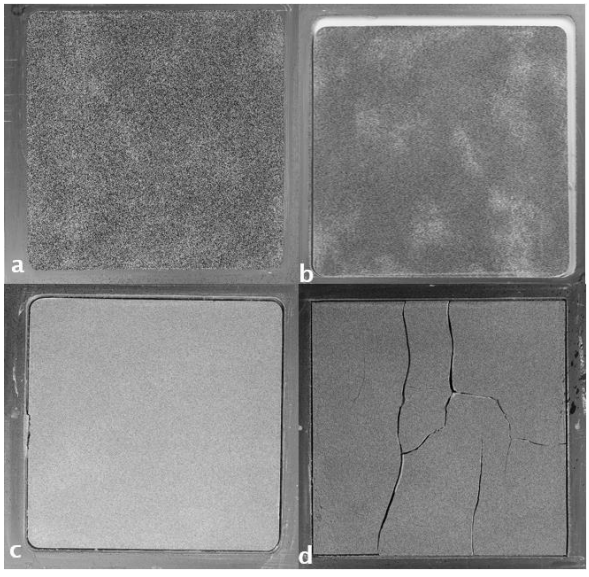

Figure 5: Desiccation of kaolinite: (a) initial state (b) final state for a smooth base (c) for a semi-rough base (d) for a rough base.

Cracking of the montmorillonite, even when friction with the support is negligible (case of the smooth base), indicates that there are other intrinsic factors that act on the montmorillonite paste by generating different types of sollicitations (compression, bending, shearing or torsion) resulting in the material breaking. In order to identify the type of solicitation present, it will be essential to complete this study with other tests by increasing the thickness of the samples, which reduces edge effects and allows better monitoring of the deformation evolution.

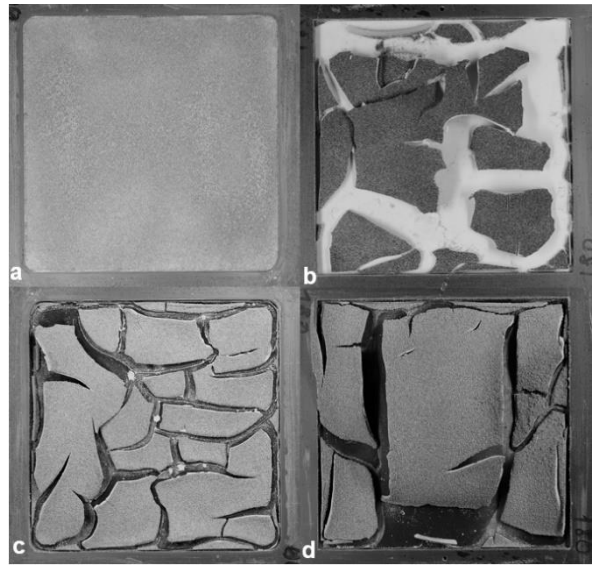

Figure 6: Desiccation of montmorillonite: (a) initial state (b) final state for a smooth base (c) for a semi-rough base (d) for a rough base.

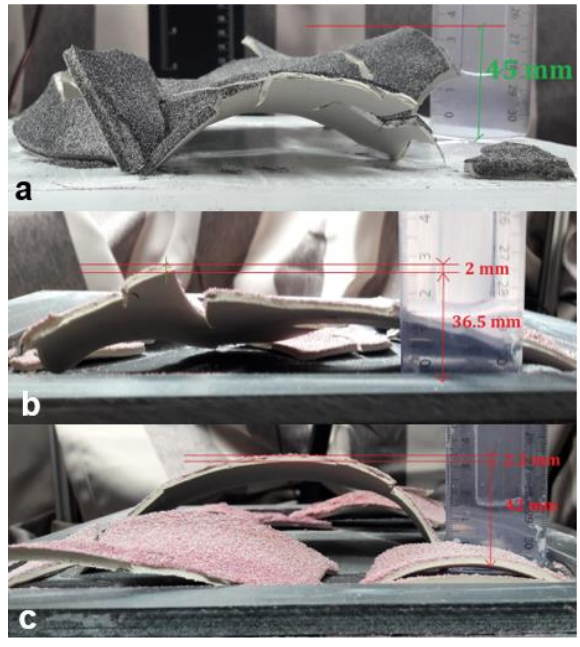

Figure 7: Deformation of montmorillonite in Z axis (a) for a smooth base (b) for a semi-rough base (c) for a rough base.

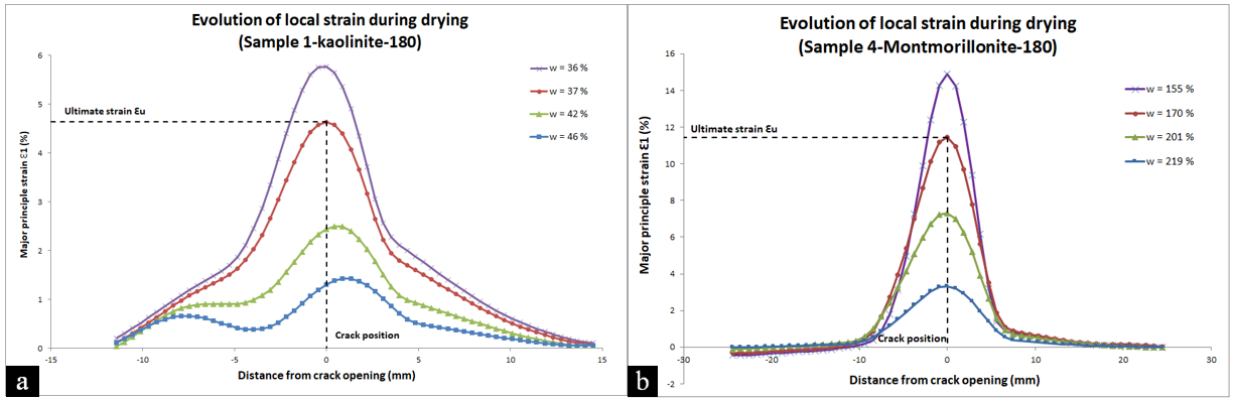

Figure 8: Evolution of local strain during drying for kaolinite (a) and montmorillonite (b) on a rough base.

Furthermore, an analysis of the porosity of the material and the orientation of the sheets at the edges of the crack and in an uncracked location will be required to analyse the influence of the discontinuity on the material failure.

By comparing the behaviour of kaolinite and montmorillonite samples poured on a rough base, we notice that the first crack appeared for a water content of 37 % in the kaolinite with a principal major deformation ε_1 = 4,6 %, and for a water content of 170 % in the montmorillonite with a principal major deformation ε_1 = 11,5 % (Figure 8).

These two deformation thresholds can therefore be defined as ultimate major deformations leading to the cracking of the material when it is subjected to tensile stress (caused by soil/base friction in this case). These results indicate that the greek calcic montmorillonite can withstand a deformation nearly twice that of the P300 kaolinite before reaching failure, although it undergoes a shrinkage twice as fast (drying slope).

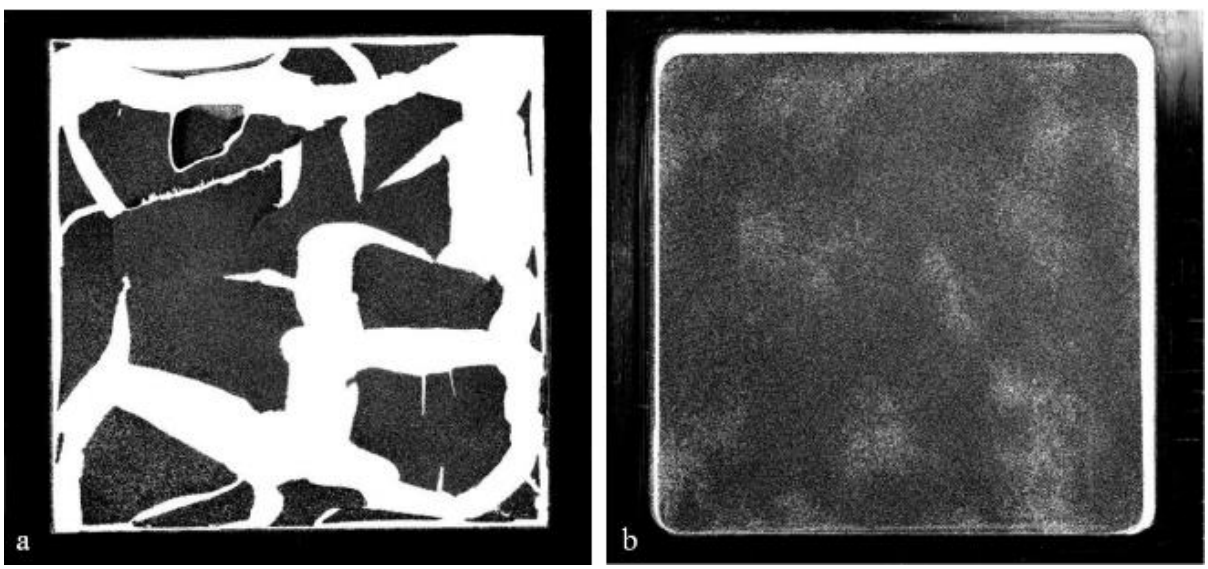

Figure 9: Deformation of montmorillonite (a) and kaolinite (b) for negligible boundary conditions.

3.2 Crack morphology

Figure 9 shows the total deformation of each sample when boundary conditions are not involved (in the case of a smooth base where the soil/base friction is negligible). It should be noted that the deformation density of montmorillonite 46 % is 7 times higher than that of kaolinite 7 %.

This difference is due to the variation between the specific surface area of each material, which implies a variation in the water adsorption rate, which explains the variation in the gap between the initial and residual water content of kaolinite (60 – 0,6 = 59,4 %) and montmorillonite (230 – 15,7 = 214,3 %). But this gap (214,3/59,4 = 3,6 times) remains even smaller than the gap of the deformation density (7 times) while keeping in mind that this calculation does not take into account the density of deformation in the Z direction which can no longer be negligible, especially in the case of a swelling clay.

This indicates that the crystallographic structure (sheet arrangement and interfoliar space thickness) influences the deformation density of the material.

4 CONCLUSION

It is quite obvious that montmorillonite has a completely different behaviour from kaolinite, it cracks even when boundary conditions do not intervene. In all cases, we have seen that the montmorillonite undergoes a significant bending with a radius of curvature that varies from 4 to 5 cm in the Z direction (Figure 7).

This difference in behavior may be due to a difference in physical properties (specific surface area 50 times higher in montmorillonite (700 to 800 m^2/g) than in kaolinite (10 to 30 m^2/g)), mineralogical properties (crystallographic structure), or chemical properties (presence of Magnesium "$Mg_{0.6}$" which causes a charge deficit in the montmorillonite).

Boundary conditions influence clay cracking, but also the intrinsic characteristics (mineralogical, mechanical and hydric) of the material have a greater influence on the cracking. Their effect can be reflected in compressive, bending, shear or tensile solicitations. Further tests must be carried out as part of this study to identify the type of solicitation that occurred.

5 REFERENCES

[1] El Hajjar A., Chauhan P., Prime N., Olivier P. 2018. Effect of suction on the mechanical characteristics of uniformly compacted rammed earth, *IOP Conference Series: Earth and Environmental Science* **143** (no. 1), 012045.

[2] Delage P., Cui Y. 2000. L'eau dans les sols non saturés, *Techniques de l'ingénieur-construction* **C 301**.

[3] Kodikara J.K., Barbour S.L., Fredlund D.G. 2000. Desiccation cracking of soil layers, *Unsaturated soils for Asia* **90** (no. 5809), 139.

[4] Fleureau J.M., Kheirbek-Saoud S., Soemitro R., Taibi S. 1993. Behavior of clayey soils on drying-wetting paths, *Canadian Geotechnical Journal* **30** (no. 2), 287–296.

[5] Hammad T. 2010. Comportement des sédiments marins de grande profondeur: approche multiéchelle, Thèse de l'Ecole Centrale de Paris, Paris.

[6] Souli H., Fleureau J.M., Ayadi M., Besnard M. 2008. Physicochemical analysis of permeability changes in the presence of zinc, *Geoderma* **145** (no. 1-2), 1–7.

[7] Eid J., Taibi S., Fleureau J.M., Hattab M. 2015. Drying, cracks and shrinkage evolution of a natural silt intended for a new earth building material: Impact of reinforcement, *Construction and Building Materials* **86**, 120–132.

[8] Wakim J. 2005. Influence des solutions aqueuses sur le comportement mécanique des roches argileuses. Thèse de l'École Nationale Supérieure des Mines de Paris, Paris.